DOI:10.1190/segam2021-3583769.1

Imaging the complex geology in the Central Basin Platform with land FWI

Dongren Bai, Lin Zheng, Wubing Deng (CGG)*

Summary

Recently, land full-waveform inversion (FWI) has shown great potential in resolving near-surface complexity in the Delaware Basin, providing significant imaging uplift and useful information for shallow hazard identification. However, deep section updates beyond diving wave penetration remain challenging.

We present an application of land FWI in the Central Basin Platform (CBP) for both shallow and deep updates. Results show that, with a time-lag cost function, a fine spatially sampled data set with proper preconditioning, and a good starting model for regions beyond diving wave penetration, land FWI was able to produce a high-resolution velocity model to resolve small-scale anomalies in the deep sections as well as detailed velocities in the near surface, leading to improved seismic images at reservoir levels. Furthermore, the impact of the FWI input data spatial sampling and the starting model in inversion are studied respectively.

Introduction

Sitting between the Delaware Basin and Midland Basin, the CBP features complex shallow evaporite deposition similar to neighboring basins, causing large near-surface velocity variation. Conventional ray-based first-arrival (FA) tomography, which relies heavily on quality first-break picks to invert for the shallow model, struggles to handle the near-surface conditions in this area mainly due to limited resolution as well as picking challenges from poor S/N of FA signals, especially in locations with severe shingling (Zhu and Cheadle, 1999). As a result, the seismic image with the shallow model from FA tomography shows structural undulation at shallow targets (YTES horizon in Figure 1b, shallow arrows).

In addition to the complex near-surface layer, a distinctive "chaotic zone" consisting of irregularly shaped, small-scale slow geobodies (blue circle in Figure 1b) exists from 5000 to 9000 ft depth. Limited by tomography resolution, reflection tomography lacks the ability to fully resolve both the small-scale anomalies and the background velocity. This causes severe structural distortion at both unconventional (WCMP) and conventional reservoir levels (MSSP), and all the way down to the basement (EBGR), which is being actively used for saltwater disposal (Figure 1b, yellow square area). Furthermore, the unidentified shallow evaporites and deep anomalies pose potential drilling hazards.

FWI has long been deemed the ultimate solution for automatic high-resolution velocity model building as it can make use of the full wavefield and discriminate small-scale anomalies. With the recent breakthroughs in FWI algorithms to address the cycle-skipping and amplitude discrepancy issues, Time-lag FWI (TLFWI) has brought a step-change to automatic velocity model building in offshore salt environments (Zhang et al., 2018), and is being routinely used in offshore projects to enable automatic salt modeling and improve subsalt imaging (Wang et al., 2019; Xue et al., 2020).

Compared to marine data, land data sets face additional challenges such as excessive noise contamination, especially surface waves, frequently poor spatial sampling with limited offset coverage, and a lack of good low-frequency signal. Thus, successful applications of land FWI remain scarce (Mei and Tong, 2015; Sedova et al., 2019; Carotti et al., 2020), especially in challenging geological settings such as the Permian Basin. (Murphy et al., 2020; Wang et al., 2020).

Recently, we achieved a successful onshore application of TLFWI primarily for the near-surface complexity in the Delaware Basin. The resulting model captured high-resolution details conformal to the near-surface geology, which not only improved the structural imaging below but also revealed important shallow hazard information. (Bai et al., 2020).

With this recent success, we took a step forward to apply land FWI top-down to a newly acquired dense CBP survey to resolve not only near-surface evaporites and anomalies, but also deep complex structure. Here we present the improved velocity model and image from shallow to deep. We also share our findings on how spatial sampling and starting model impact land FWI results.

A dense survey in the Permian Basin

The land seismic survey in this study was recently acquired in the CBP area using a low dwell broadband sweep from 2 to 96 Hz. The acquisition parameters are significantly denser than the typical acquisitions in the Permian Basin, featuring an 82.5 ft station interval, a 495 ft line interval, and a maximum offset of ~23000 ft. As a result, this survey is more than 10 times denser than typical spec acquisitions in the area, which usually have 165 ft station interval and 825/990 ft line interval.

Time-lag FWI to resolve shallow and deep structure

As commonly seen in the Permian Basin, this raw data is dominated by various types of noise, most notably surface wave energy (Figure 2a). Since current acoustic FWI is unable to model surface waves, a fit-for-purpose data preconditioning flow was applied to attenuate these energies. A shot gather example after preconditioning shows that the S/N has been improved from shallow to deep and from near to far offsets (Figure 2c). This, together with an effective direct arrival artifact suppression approach implemented on the FWI modeling side (Wang et al., 2020), eliminates the need to mute particular arrivals and thus ensures both diving waves and reflections are included in the inversion.

With a maximum offset of ~23000 ft and a relatively large shallow velocity gradient, the diving wave penetration is limited to only ~5000 ft. Therefore, the deep update from TLFWI, including the chaotic zone (blue circle in Figure 1b), relied mostly on reflection energy, which is incapable of resolving the background velocity errors (Wang et al., 2019). For these reasons, ray-based reflection tomography and well calibration were still required to improve the top-down background velocity prior to TLFWI. Following the conventional velocity model building flow, the initial model was first built from the near-surface model obtained from FA tomography and sonic logs of available wells, and then followed by reflection tomography update and well calibration. The resulting VTI model provided a good low-wavenumber background velocity, as indicated by the reasonable gather flatness and well tie, and thus was used as the input model to FWI (Figures 1a-1c).

Running TLFWI from 5 Hz to 12 Hz using both diving wave and reflection energy was able to capture the complex shallow evaporites (Figure 3d), small-scale slow anomalies, and dipping structures (Figure 1d). This more geologically conformal velocity model led to improved images and gathers. Kirchhoff migration images show that both the shallow YTES target and deep WCMP/MSSP/EBGR targets become more focused and simplified with the detailed FWI model (Figures 1b and 1e). On the gather examples (Figures 1c and 1f), in addition to the flattened shallow events, the obvious non-hyperbolic moveout caused by the unresolved small-scale anomalies in the input model was fixed with FWI and event coherency was enhanced.

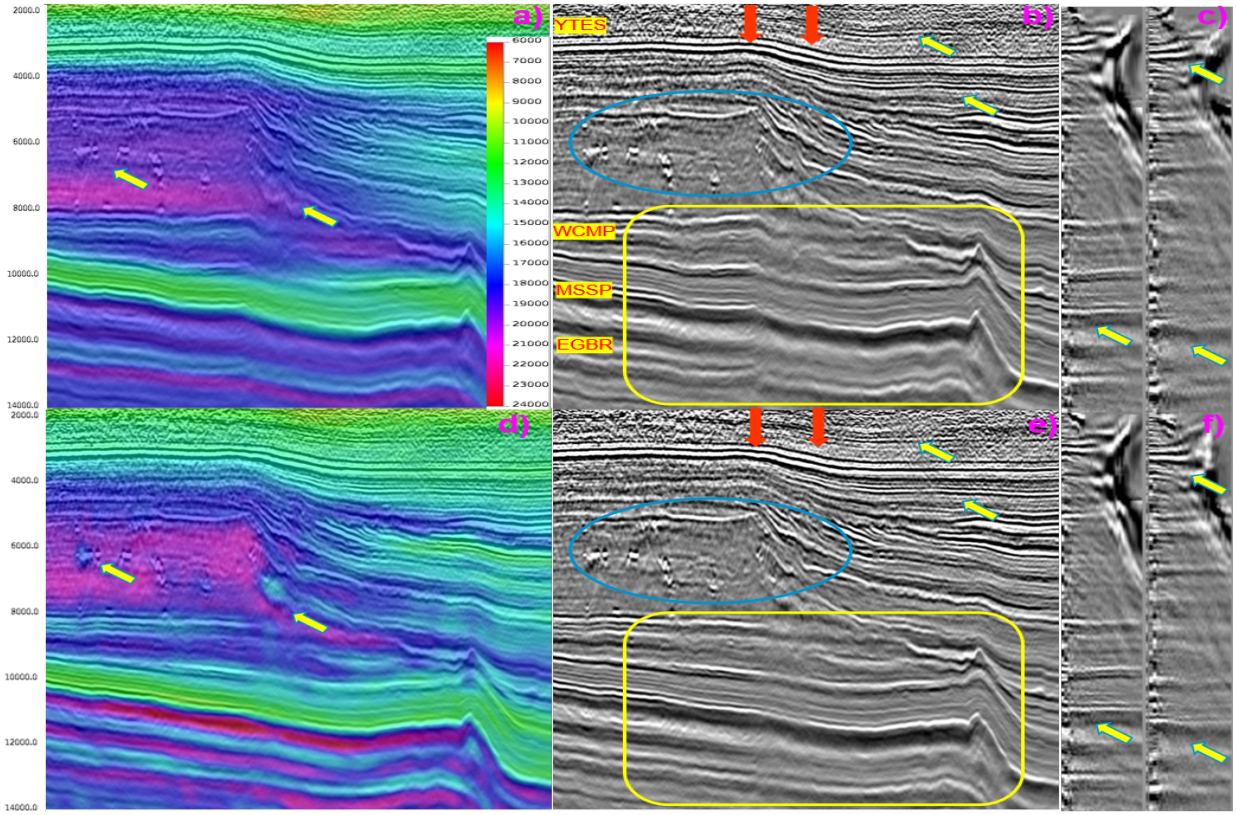

Figure 1: Starting model: a) model, b) stack, c) gathers corresponding to the two red arrow locations on the stack. 12 Hz FWI model: d) model, e) stack, f) gathers. The 12 Hz FWI captures the fine details in the model, leading to image uplift in the circled area and flattened CIG gathers. YTES/WCMP/MSSP/EGBR refer to Yates/Wolfcamp/Mississippian/Ellenburger, respectively.

How spatial sampling affects land FWI

This survey was acquired to be more than 10 times denser than a typical seismic survey in the Permian Basin, with the aim of obtaining a better FWI update and improved seismic imaging. Given the dense CBP acquisition, a test was conducted to use decimated data as input to FWI to evaluate the benefit of the fine spatial sampling.

For the purpose of proper evaluation, the raw data was first decimated by dropping every other station and line to simulate a typical spec acquisition geometry of 165 ft station interval and 990 ft line interval. While diving waves and reflections remained well sampled after decimation, the dipping surface wave energy became spatially aliased due to its slow velocity (Figures 2e and 2f).

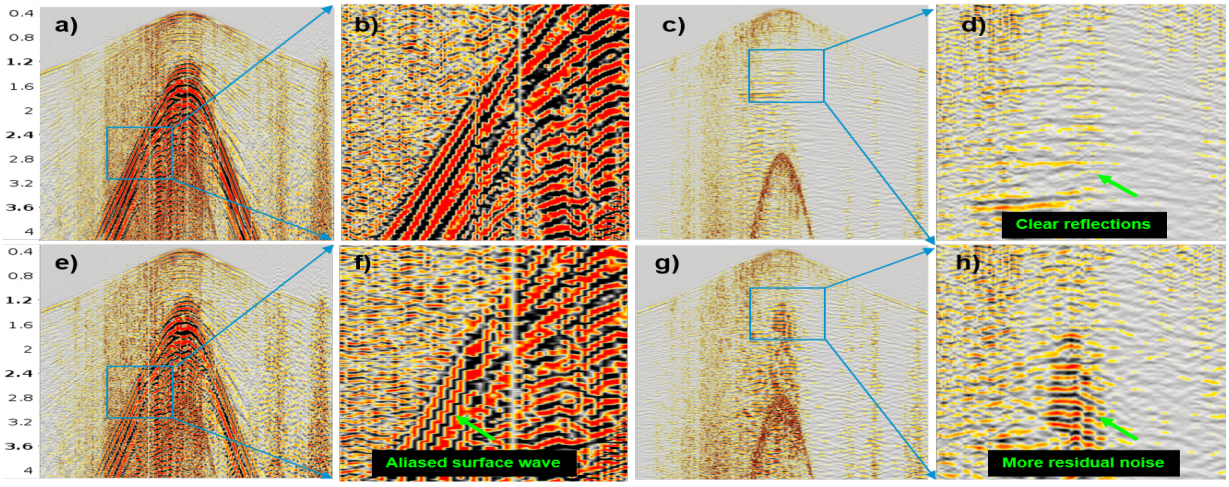

Figure 2: Dense input preconditioning: a) original dense raw gather, b) zoomed in on surface wave, c) dense gather after preconditioning, d) zoom in on reflections. Decimated input preconditioning: e) decimated raw gather, f) zoom in on surface wave, g) decimated gather after preconditioning, h) zoom in on reflections. Note the aliased surface wave on the input and more residual noise on the output with decimated input test.

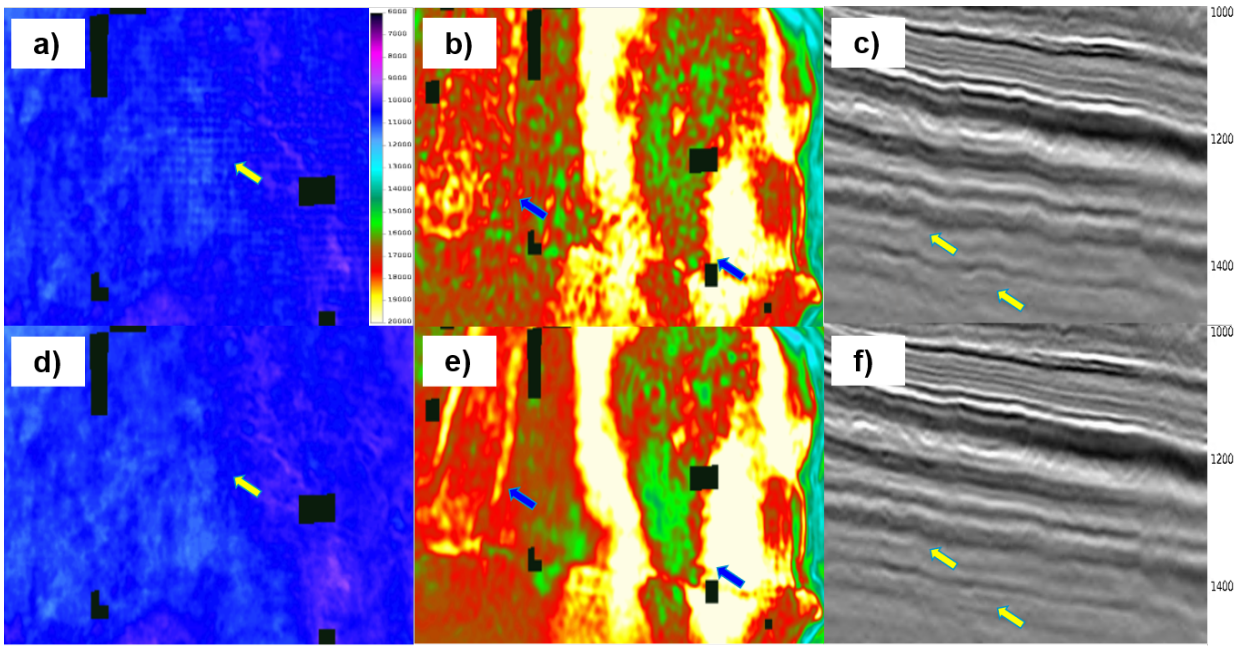

Figure 3: FWI with decimated input: a) model at 1600 ft, b) model at 12000 ft, c) stack. FWI with original dense input: d) model at 1600 ft, e) model at 12000 ft, f) stack. Strong footprint, noisier update, and more structural distortion can be observed with the decimated input.

The decimated data was then put through the same data preconditioning flow used for the non-decimated data, with parameters adjusted according to the coarser station/line intervals. While the denoise algorithm effectively attenuated most of the surface waves by mitigating the aliasing impact (Le Meur et al., 2008), there was much more residual noise masking near to middle offset reflections on the decimated result (Figures 2d and 2h). This indicates that advanced noise attenuation algorithms can address the spatial aliasing to some extent but cannot fully resolve it, and the densely acquired field data is still essential.

Compared with the 12 Hz FWI model using non-decimated input data, the 12 Hz FWI model from the decimated input shows a less coherent shallow update with strong footprint (Figures 3a and 3d) as a result of the larger station/line intervals. In the deep section (Figures 3b and 3e), the update appears to be poorly defined and much noisier due to the lower stacking power of the reduced number of traces and noisier input data. As expected, this noisy model resulted in more structural undulation along deep targets (Figures 3c and 3f).

The decimation test demonstrates how fine spatial sampling benefits FWI in terms of: less footprint, more geologically conformal velocity model, cleaner update from higher stacking power, and better denoised data.

How important is the starting model for land FWI

The lack of diving wave constraints for the deep sections significantly increases the chance of cycle-skipping, which prompted us to look further into the impact of the starting model.

One FWI test was carried out with the same inversion scheme but a poor starting model, that is prior to the reflection tomography update, and shows obvious residual gather curvature from shallow to deep (Figure 4a). Compared with the FWI result using a better starting model incorporating reflection tomography and well calibration, the FWI result from the poor starting model shows a very similar update within the diving wave penetration zone above 5000 ft, which confirms that the FWI update driven primarily by diving waves is less sensitive to the starting model accuracy. However, the deep update beyond 5000 ft relies mostly on reflection energy, which is incapable of resolving the background velocity errors. Consequently, the two models display very different trends in the deep, with the FWI model from the poor starting model exhibiting a clearly reversed trend from the well sonic log (deep arrow in Figure 4c and 4g), which resulted in worse gather flatness (Figure 4d and 4h).

Based on the test outlined above, we could conclude that, due to the limited diving wave penetration depth from the limited maximum offset, a starting model from a conventional velocity update flow is still necessary for land FWI to reliably update from shallow to deep, especially beyond the diving wave penetration zone.

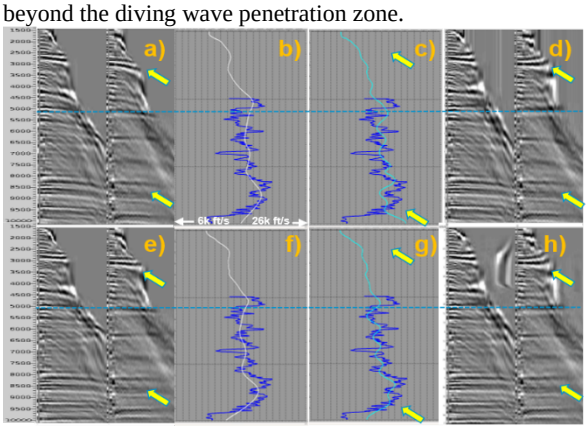

Figure 4: FWI with poor starting model: a) starting model gathers around well location, b) starting velocity (white) overlaid on the sonic log (blue), c) FWI velocity (cyan) overlaid on the sonic log (blue), d) FWI model gathers around the well location. FWI with good starting model: e) starting model gathers, f) starting velocity overlaid on the sonic log, g) FWI velocity overlaid on the sonic log, h) FWI model gathers around the well location. The blue dotted line corresponds to the diving wave penetration depth of ~5000 ft. The two FWI models are very similar above 5000 ft but show very different trends in the deeper sections.

Discussion and conclusions

We demonstrated that land FWI is able to resolve the near surface and deep velocity complexities in the CBP area, thus improving seismic imaging at the reservoir levels. The TLFWI cost function, a fine spatially sampled data set with proper preconditioning, and a good starting model are crucial for obtaining reliable and consistent updates from shallow to deep.

However, it is important to recognize that land FWI in general remains very challenging, mainly due to: coarsely sampled data lacking very near and far offsets, poor low-frequency signal, and insufficient physics of the current acoustic modeling engine failing to account for elastic effects.

Acknowledgments

We thank CGG Multi-Client for permission to publish this work. We are grateful to numerous CGG colleagues, especially Rachel Gong and Chi Chen for pioneer testing, Amin Baharvand for data preparation, and Jiawei Mei, Yan Huang, and Shuang Sun for fruitful discussions.

References

Bai, D., F. Hou, and J. Hefti, 2020, A case study in the Delaware Basin: Application of Time-Lag FWI and 3D SRME/IMA multiple attenuation: Geoconvention 2020, CSEG, Expanded Abstracts.

Carotti, D., O. Hermant, S. Masclet, M. Reinier, J. Messud, A. Sedova, and G. Lambaré, 2020, Optimal transport full waveform inversion – Applications: 2020 Conference and Exhibition Online, EAGE, Extended Abstracts, 1–5, doi: https://doi.org/10.3997/2214-4609.202011288.

Le Meur, D., N. Benjamin, R. Cole, and M. Al Harthy, 2008, Adaptive Groundroll Filtering: 70th Conference and Exhibition, EAGE, Extended Abstracts, G036, doi: https://doi.org/10.3997/2214-4609.20147745.

Mei, J., and Q. Tong, 2015, A practical acoustic full waveform inversion workflow applied to a 3D land dynamite survey: 85th Annual International Meeting, SEG, Expanded Abstracts, 1220–1224, doi: https://doi.org/10.1190/segam2015-5850377.1.

Murphy, G., V. Brown, and D. Vigh, 2020, Land FWI in the Delaware Basin, west Texas: A case study: The Leading Edge, **39**, 324–331, doi: https://doi.org/10.1190/tle39050324.1.

Sedova, A., G. Royle, T. Allemand, G. Lambaré, and O. Hermant, 2019, High-frequency acoustic land full-waveform inversion: A case study from the Sultanate of Oman: First Break, **37**, 75–81, doi: https://doi.org/10.3997/1365-2397.n0010.

Wang, D., C. Chen, D. Zhuang, J. Mei, and P. Wang, 2020, Land FWI: Challenges and possibilities: 82nd Conference and Exhibition, EAGE, Extended Abstracts, Jul 2020, Volume **2020**, 1–5, doi: https://doi.org/10.3997/2214-4609.202011175.

Wang, P., Z. Zhang, J. Mei, F. Lin, and R. Huang, 2019, Full-waveform inversion for salt: A coming of age: The Leading Edge, **38**, 204–213, doi: https://doi.org/10.1190/tle38030204.1.

Xue, Z., Z. Zhang, F. Lin, J. Mei, R. Huang, and P. Wang, 2020, Full-waveform inversion for sparse OBN data: 90th Annual International Meeting, SEG, Expanded Abstracts, 686–690, doi: https://doi.org/10.1190/segam2020-3427891.1.

Zhang, Z., J. Mei, F. Lin, R. Huang, and P. Wang, 2018, Correcting for salt misinterpretation with full-waveform inversion: 88th Annual International Meeting, SEG, Expanded Abstracts, 1143–1147, doi: https://doi.org/10.1190/segam2018-2997711.1.

Zhu, T. F, and S. Cheadle, 1999, A grid ray-tracing method for near-surface traveltime modeling: 79th Annual International Meeting, SEG, Expanded Abstracts, 1759–1762, doi: https://doi.org/10.1190/1.1820877.